

Genomic Binding Patterns of Forkhead Box Protein O1 Reveal Its Unique Role in Cardiac Hypertrophy

BACKGROUND: Cardiac hypertrophic growth is mediated by robust changes in gene expression and changes that underlie the increase in cardiomyocyte size. The former is regulated by RNA polymerase II (pol II) de novo recruitment or loss; the latter involves incremental increases in the transcriptional elongation activity of pol II that is preassembled at the transcription start site. The differential regulation of these distinct processes by transcription factors remains unknown. Forkhead box protein O1 (FoxO1) is an insulin-sensitive transcription factor that is also regulated by hypertrophic stimuli in the heart. However, the scope of its gene regulation remains unexplored.

METHODS: To address this, we performed FoxO1 chromatin immunoprecipitation–deep sequencing in mouse hearts after 7 days of isoproterenol injections (3 mg·kg⁻¹·mg⁻¹), transverse aortic constriction, or vehicle injection/sham surgery.

RESULTS: Our data demonstrate increases in FoxO1 chromatin binding during cardiac hypertrophic growth, which positively correlate with extent of hypertrophy. To assess the role of FoxO1 on pol II dynamics and gene expression, the FoxO1 chromatin immunoprecipitation–deep sequencing results were aligned with those of pol II chromatin immunoprecipitation–deep sequencing across the chromosomal coordinates of sham- or transverse aortic constriction–operated mouse hearts. This uncovered that FoxO1 binds to the promoters of 60% of cardiac-expressed genes at baseline and 91% after transverse aortic constriction. FoxO1 binding is increased in genes regulated by pol II de novo recruitment, loss, or pause-release. In vitro, endothelin-1– and, in vivo, pressure overload–induced cardiomyocyte hypertrophic growth is prevented with FoxO1 knockdown or deletion, which was accompanied by reductions in inducible genes, including *Comtd1* in vitro and *Fstl1* and *Uck2* in vivo.

CONCLUSIONS: Together, our data suggest that FoxO1 may mediate cardiac hypertrophic growth via regulation of pol II de novo recruitment and pause-release; the latter represents the majority (59%) of FoxO1-bound, pol II–regulated genes after pressure overload. These findings demonstrate the breadth of transcriptional regulation by FoxO1 during cardiac hypertrophy, information that is essential for its therapeutic targeting.

Jessica Pflieger, PhD
Ryan C. Coleman, PhD
Jessica Ibeti^{ID}, PhD
Rajika Roy, PhD
Ioannis D. Kyriazis^{ID}, PhD
Erhe Gao, MD, PhD
Konstantinos Drosatos^{ID}, PhD
Walter J. Koch^{ID}, PhD

Key Words: cardiomegaly ■ chromatin immunoprecipitation sequencing ■ endothelin-1 ■ Forkhead box protein O1 ■ gene expression ■ RNA polymerase II ■ transcription, genetic

Sources of Funding, see page 897

© 2020 American Heart Association, Inc.

<https://www.ahajournals.org/journal/circ>

Clinical Perspective

What Is New?

- This study is the first to demonstrate that FoxO1 (forkhead box protein O1) genomic binding is widespread in both the healthy and diseased heart and increases during pathological hypertrophic growth.
- This is also the first study to show that cardiac FoxO1 knockdown or deletion prevents hypertrophic growth induced by pressure overload.
- Together, the data suggest that FoxO1 may contribute to cardiac hypertrophic growth via the regulation of RNA polymerase II de novo recruitment and pause-release, or the regulation of inducible and essential, incrementally increased genes.

What Are the Clinical Implications?

- These findings challenge the therapeutic targeting of FoxO1 during pathological cardiac hypertrophy because it may regulate the transcription of a subset of inducible genes, as well as a subset of incrementally increased genes, that underlie adaptive cardiac growth.
- This study underscores the necessity for understanding the full spectrum of targets and functions of transcription factors for their clinical targeting.

Alterations in gene expression are essential to the molecular mechanisms that drive cardiac hypertrophic growth. These include robust upregulation or downregulation of certain genes, for example, those involved in fetal gene reprogramming.¹ In addition to these substantial changes, there are underlying increases in the expression of the vast majority of cardiac-expressed genes that are essential to match the increase in cardiomyocyte size.² These include, for example, certain metabolic enzymes, ion channel constituents, and cell surface proteins. The distinction between these categories of genes becomes critical when designing novel therapies directed at transcriptional machinery, which is of much interest. Inhibition of general transcription factor IIB,³ histone deacetylases,^{4,5} and bromodomain-containing protein 4 (Brd4),⁶ to name a few examples, has proved beneficial for the attenuation of cardiac hypertrophy in mouse models. Moreover, loss of prohypertrophic transcription factors such as MEF2D⁷ or gain of antihypertrophic transcription factors such as forkhead box protein (Fox) O1 or 3⁸ also prevents pathological hypertrophic growth. It remains important, however, to understand the scope of these transcription regulators and the mechanisms by which they target various gene subsets during physiology and pathology. This information is critical as we aim to inhibit pathological gene expression while sparing adaptive growth.

Variations in RNA polymerase II (pol II) recruitment and elongation distinguish between upregulated or downregulated genes and incrementally increased genes during cardiac hypertrophy.² Those that are upregulated are defined as having de novo pol II recruitment to the transcription start site (TSS) and gene body. Conversely, those that are downregulated have loss of pol II in these gene regions. Those that are incrementally increased to parallel an increase in cardiomyocyte size are regulated by pol II pause-release.² Specifically, paused pol II describes preassembled pol II at the TSS under basal conditions. On induction of hypertrophy, this paused pol II is released into the gene body to increase transcription concurrent with growth.^{2,9} Pol II pausing is widespread in the heart, and >50% of genes are reported to be regulated by pause-release after hypertrophy.² In general, pause-release is thought to rapidly and synchronously regulate transcription in response to various stimuli.⁹ In fact, pause-release has been shown to drive gene expression in *Drosophila melanogaster* in response to heat shock^{10,11} and in human colorectal cancer cells in response to hypoxia.¹² Thus, it is presumed that cardiac paused pol II will be released in response to numerous stimuli, yet the extent, loci specificity, and functionality have yet to be determined. Moreover, the signals that differentially drive pol II de novo recruitment, loss, and pause-release, especially in the heart during physiological and pathophysiological growth, remain unclear. Again, understanding these differences is central for novel transcriptional therapeutic strategies.

As mentioned, FoxO1 is a transcription factor that has been shown to be antihypertrophic, largely via its activation of atrophic genes such as *Fbxo32*. Immediate stimulation with hypertrophic agonists yields FoxO1 nuclear export, preventing *Fbxo32* transcription and leading to a hypertrophic phenotype in cardiomyocytes.^{8,13} *Fbxo32* encodes atrogin-1, an E3 ubiquitin ligase, which also has been shown to target and inhibit calcineurin and therefore downstream hypertrophic nuclear factor of activated T cells activity. Thus, its loss stabilizes calcineurin/nuclear factor of activated T cells signaling and hypertrophy.⁸ In addition, FoxO1 overexpression prevented angiotensin II-mediated cardiomyocyte hypertrophy.⁸ Accordingly, FoxO1 has been proposed as a therapeutic target for hypertrophic cardiomyopathies. However, the localization and function of FoxO1 after more chronic hypertrophic stress, with desensitization of the receptors that mediate its upstream signaling, are unknown. Furthermore, the scope and patterns of FoxO1 binding during basal and hypertrophic conditions are also unknown. Addressing these gaps in knowledge is critical for targeting transcription factors such as FoxO1. Thus, they were the focus of our study.

Through genome-wide analyses, we uncovered the widespread binding of FoxO1 and its indiscrimination

with regard to differential pol II regulation during cardiac hypertrophy. This work is noteworthy as it challenges the notion of FoxO1 as a desirable therapeutic target under these conditions. Consistently, it underscores the value of understanding the scope and mechanistic effects of other transcription factors and machinery for their therapeutic targeting.

METHODS

The methods and materials used for these studies and the data generated will be made available to researchers seeking to replicate the procedures or results. The raw and unprocessed FoxO1 chromatin immunoprecipitation followed by deep sequencing (ChIP-Seq) data have been deposited into Gene Expression Omnibus (GSE144011). All animal procedures were performed in accordance with the National Institutes of Health *Guide for the Care and Use of Laboratory Animals*. All animal protocols were approved by the Institutional Animal Care and Use Committee of Temple University. Detailed methods can be found in the [Data Supplement](#).

Statistical Analyses.

Significant differences between the means of 2 sample groups were calculated with *t* tests (equal variance, 2 tailed), and 1- or 2-way ANOVA with Tukey post hoc testing was used for multiple comparisons. Values of $P < 0.05$ were considered as significant.

RESULTS

FoxO1 Chromatin Binding Positively Correlates With Cardiac Hypertrophy

To begin to understand the role of FoxO1 in cardiac hypertrophy, we examined its nuclear localization and binding to the cardiac genome. For this, we subjected wild-type (WT) C57Bl/6 mice to sham operation and vehicle injections, isoproterenol injections ($3 \text{ mg} \cdot \text{kg}^{-1} \cdot \text{mg}^{-1}$), or transverse aortic constriction (TAC) over 7 days. Isoproterenol-treated and TAC hearts were hypertrophic at 7 days, as indicated by a significant increase in heart weight-to-body weight (HW/BW) ratios (15.9% and 25.4%, respectively; Figure 1A). However, there were no significant differences in cardiac function, as determined by echocardiographic analyses of ejection fraction and fractional shortening, between any of the tested groups (Figure 1A and 1B in the [Data Supplement](#)). Success and consistency of TAC were confirmed by significant increases in aortic mean (2.8-fold) and peak (11.4-fold) pressure gradients versus sham-operated mice (Figure 1C in the [Data Supplement](#)). Moreover, there were no significant differences in serum insulin or blood glucose levels (Figure 1B and 1C). Subcellular fractionation and Western blotting were then performed, and no significant difference in nuclear

or cytosolic FoxO1 was observed in any of the tested groups (Figure 1D and 1E). As a positive control for nuclear-to-cytosolic shuttling, mouse hearts were fractionated, and Western blotting for FoxO1 was performed after 1 hour of vehicle or insulin (1 U/kg) stimulation (Figure 1A in the [Data Supplement](#)). To examine FoxO1 genomic binding, we performed ChIP-Seq for FoxO1 in murine hearts 7 days after sham operation/vehicle treatment, isoproterenol treatment, or TAC. The data reveal an increase in the total amount of FoxO1 binding across the genome (total sequence tags) in hearts after isoproterenol treatment (52.4%) or TAC (56.5%). However, there are decreases in the total number of FoxO1-bound regions (filtered peaks or merged regions) after isoproterenol treatment (27.7% or 26.6%, respectively) or TAC (6.5% or 8.3%, respectively), suggesting a rearrangement and enrichment of chromatin-bound FoxO1 peaks under these conditions (Table 1 in the [Data Supplement](#)). We next examined the extent of FoxO1 binding at these FoxO1-bound regions (merged regions) and observed an increase in the median average peak value at these sites with isoproterenol (20.8%) or TAC (37.6%) versus sham/vehicle control hearts (Figure 1F). This corresponded to significant increases in the mean of the average peak values at these sites with isoproterenol (21.5%) or TAC (35.2%) versus sham/vehicle control (Figure 1G). Notably, the extent of binding positively correlates with HW/BW. This increase in FoxO1 binding was confirmed in chromatin fractions from neonatal rat ventricular cardiomyocytes with adenoviral expression of FoxO1 and treatment with vehicle or isoproterenol ($10 \text{ } \mu\text{mol/L}$) at 0 and 24 hours, with collection at 48 hours (Figure 1H and 1I). Consistently, we observed reductions in FoxO1 phosphorylation at serine 256 in murine hearts after isoproterenol treatment (78.6%) or TAC (69.2%; Figure 1J and 1K). Phosphorylation of FoxO1 at serine 256 has been shown to reduce its DNA-binding affinity.¹⁴ Together, these data demonstrate that although there is no detectable nuclear-to-cytosolic shuttling of FoxO1 under hypertrophic conditions, there are alterations in its chromatin binding. Specifically, an increase in FoxO1 binding correlates with increased cardiac hypertrophic growth.

FoxO1 Is Detected Primarily at the TSS of Genes

In addition to the extent of FoxO1 binding, the ChIP-Seq results provide spatial data for its binding. For the first time, we demonstrate that FoxO1 binding is widespread; peaks were observed in promoter (-1000 to -10000 base pairs [bp] relative to the TSS), TSS (-1000 to $+1000$ bp relative to the TSS), in-gene, and intergenic regions. Sixty-three percent of FoxO1-bound regions

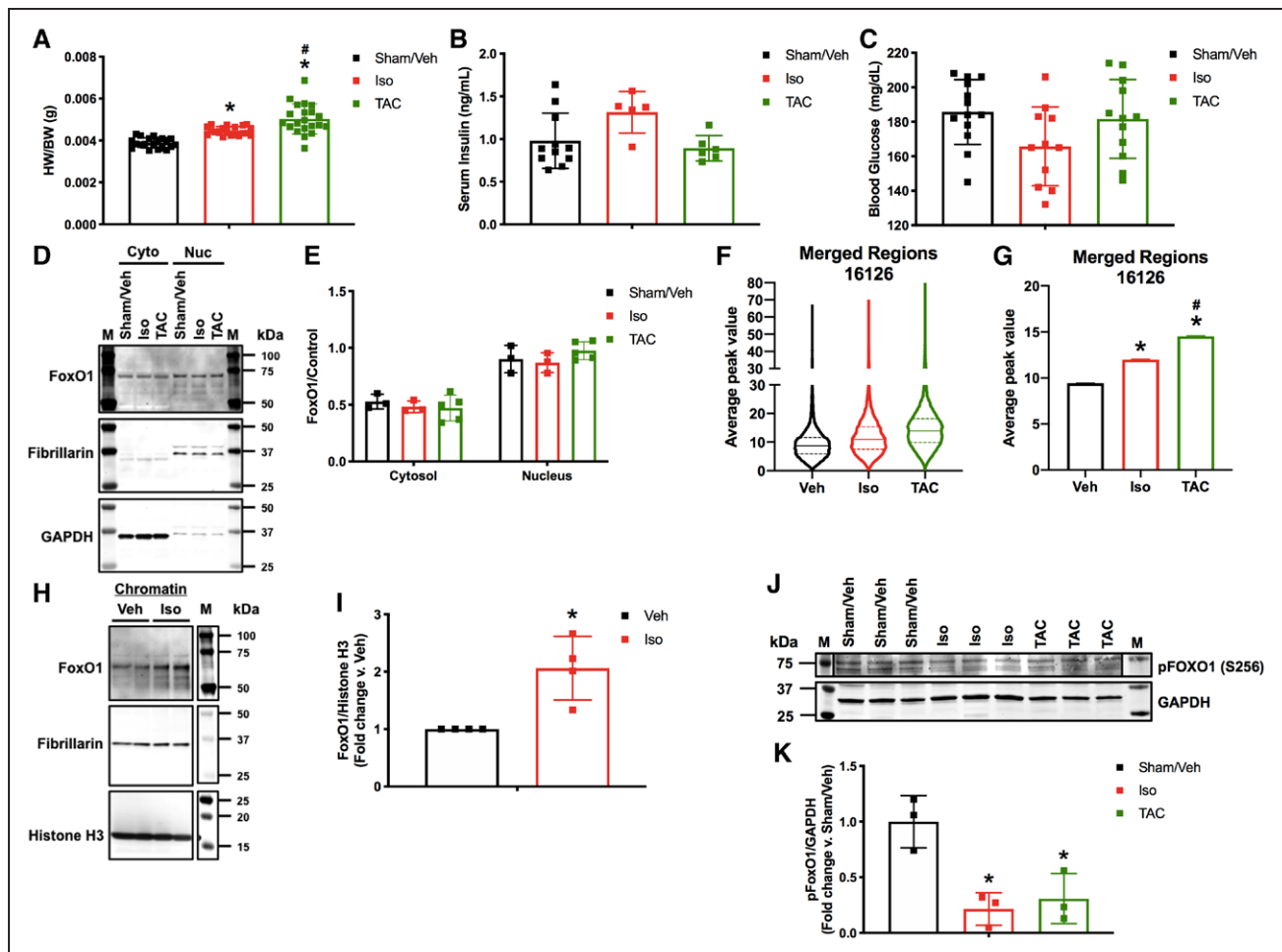


Figure 1. Forkhead box protein O1 (FoxO1) chromatin binding positively correlates with cardiac hypertrophy.

Adult (12-week-old) male C57Bl/6 mice were treated with isoproterenol (Iso; 3 mg·kg⁻¹·mg⁻¹) or subjected to transverse aortic constriction (TAC) surgery for 7 days. Controls were sham-operated and injected with vehicle (Sham/Veh) for 7 days. **A**, Hearts were harvested and weighed. Heart weights (HW) were normalized to body weights (BW) and plotted as a ratio in grams. n=20, 20, 21 (Sham, Iso, TAC). **B**, Serum insulin levels were assessed with ELISA for mouse insulin. Concentrations are plotted as nanograms per milliliter. n=7, 7, 4 (Sham, Iso, TAC). **C**, Blood glucose levels were assessed with a glucose meter. Concentrations are plotted as milligrams per deciliter. n=13, 11, 12 (Sham, Iso, TAC). **D** and **E**, Hearts were harvested and lysed, and the cytosolic (Cyto) or nuclear (Nuc) fractions were extracted. Lysates were subjected to Western blotting with the indicated antibodies. Signals from the different proteins were quantified with densitometry, normalized to loading controls (GAPDH or fibrillarlin for cytosolic or nuclear fractions, respectively) and plotted. n=3, 3, 5 (Sham, Iso, TAC). **F** and **G**, Five hearts per group (Sham/Veh, Iso, TAC) were pooled, fixed, processed for chromatin extraction, and subjected to FoxO1 chromatin immunoprecipitation followed by deep sequencing. Average peak values were plotted for all merged regions and presented as violin plots showing the median, quartiles, and distribution (**F**) or as bar graphs representing the mean (**G**). **H** and **I**, Neonatal rat ventricular cardiomyocytes were cultured, infected with Ad.FoxO1 (multiplicity of infection=1), and treated with 10 μmol/L Iso or Veh control at 0 and 24 hours. Chromatin fractions were extracted at 48 hours and subjected to Western blotting with the indicated antibodies. Signals from the different proteins were quantified with densitometry, and FoxO1 was normalized to histone H3 and plotted as fold change vs Veh. n=4, 4 (Veh, Iso). **J** and **K**, Hearts were harvested, lysed, and subjected to Western blotting with the indicated antibodies. Signals from the different proteins were quantified with densitometry, normalized to the GAPDH loading control, and plotted. n=3, 3, 3 (Sham, Iso, TAC). Error bars represent SEM. M indicates marker. **P*<0.05 Iso or TAC vs Sham/Veh, #*P*<0.05 TAC vs Iso, 1-way ANOVA. **P*<0.05 Iso vs Veh, *t* test.

were at TSS versus 21%, 27%, and 12% for promoter, in-gene, and intergenic regions, respectively (Figure 2A through 2D). Moreover, there were increases in the median and mean average peak values in the isoproterenol or TAC group versus sham/vehicle controls in each genomic region (Figure 2A through 2D and Figure IIIA through IIID in the Data Supplement). It is important to note that although there was an overall increase in FoxO1 binding with cardiac hypertrophy, there were subsets of genes with decreased binding after isoproterenol treatment or TAC in each genomic region (Figures IV through VII in the Data Supplement). These

subsets, however, represent small fractions (12%, 16%, 11%, and 9% in promoter, TSS, in-gene, and intergenic regions, respectively) of the total amount of FoxO1 bound to each region for isoproterenol-treated hearts. This compares with 50%, 40%, 60%, and 64%, respectively, that have increased FoxO1 binding (Figures IV and V in the Data Supplement). After TAC, there is a greater disproportion between those genes with decreased (6%, 6%, 7%, and 11%, respectively) versus increased (74%, 69%, 71%, and 63%, respectively) FoxO1 binding (Figures VI and VII in the Data Supplement). In specific examinations of the TSS-containing

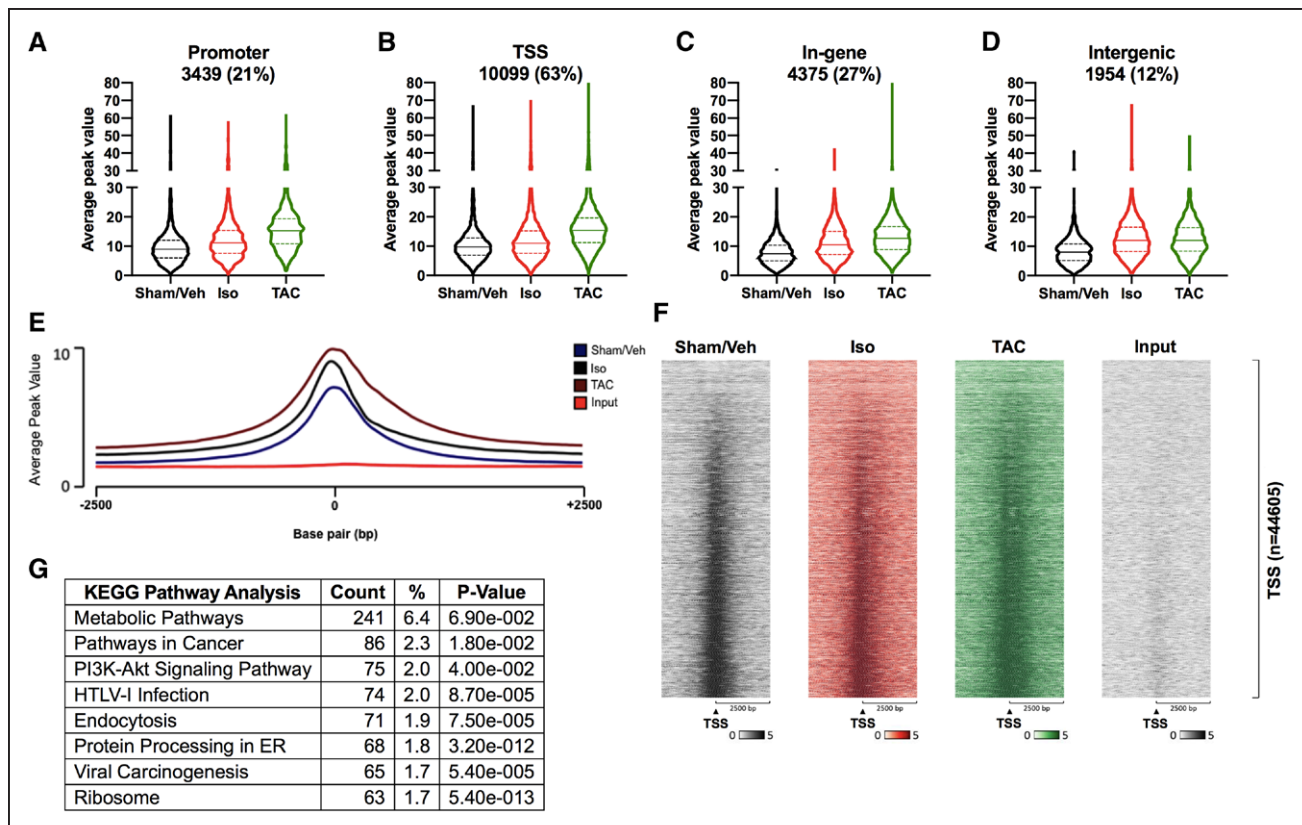


Figure 2. Forkhead box protein O1 (FoxO1) is detected primarily at transcription start sites of genes.

FoxO1 chromatin immunoprecipitation followed by deep sequencing was performed as described in Figure 1. **A** through **D**, FoxO1-bound merged regions were sorted by genomic region. Promoter represents -1000 to -10000 base pair (bp) relative to the transcription start site (TSS). TSS represents -1000 to 1000 bp relative to the TSS. Intergenic represents those not represented in the promoter, TSS, or in-gene. Average peak values were plotted and presented as violin plots showing the median, quartiles, and distribution. Percentages represent the fraction of FoxO1 bound to a particular genomic region relative to all of the FoxO1-bound merged regions (16 126). Merged regions can be present in ≥ 1 genomic regions. **E**, Average peak values (y axis) were plotted vs sequencing tags across the TSS (-2500 to $+2500$ bp relative to the TSS; x axis; EaSeq software). **F**, Sequencing tags distribution (y axis) across the TSS (-2500 to $+2500$ bp relative to the TSS; x axis) is presented as heatmaps. **G**, KEGG pathway enrichment analysis was performed with the Database for Annotation, Visualization, and Integrated Discovery for the merged regions containing FoxO1 at the TSS (**B**), sham/vehicle (Veh), isoproterenol (Iso), and transverse aortic constriction (TAC). Shown are the top 8 most highly represented pathways. ER indicates endoplasmic reticulum; HTLV-1, human T-cell leukemia virus 1; and PI3K, phosphatidylinositol 3-kinase.

region, which had the highest percentage of FoxO1 binding, it was evident that the majority of binding occurred at the TSS (Figure 2E and 2F). TSS binding of FoxO1 also increased with isoproterenol treatment or TAC and positively correlated with HW/BW (Figure 2E and 2F). KEGG pathway enrichment analyses were also performed for genes with TSS-bound FoxO1 and showed that genes involved in metabolism were the most highly represented (Figure 2G and Table II in the Data Supplement). In addition, to confirm the specificity of FoxO1 binding during hypertrophy, genes with increased binding after isoproterenol treatment or TAC were compared and show significant overlap. Specifically, 76.7%, 82.7%, and 52% of genes with increased FoxO1 binding after isoproterenol treatment are shared with those after TAC in promoter, TSS, and in-gene regions, respectively (Figure VIII in the Data Supplement). Moreover, pathway analyses of these overlapping genes with TSS-bound FoxO1 reveal metabolic pathways as the most highly represented term (Table III in the Data Supplement). Overall, these data demonstrate

that FoxO1 is detected primarily at the TSS of genes, where it increases with cardiac hypertrophy.

To further understand the nature of FoxO1 binding in our ChIP-Seq studies, motif analyses were performed for the promoter, TSS, in-gene, and intergenic regions in our sham/vehicle, isoproterenol, or TAC data sets. The results reveal the discovery of Fox motifs within the top 2 identified de novo motifs in the promoter, in-gene, and intergenic regions of the sham/vehicle, isoproterenol, and TAC data sets. No Fox motifs were identified, however, at the TSS of any of these groups (Table 1). These data suggest direct binding of FoxO1 at the promoter, in-gene, and intergenic regions and indirect binding at the TSS. This is not surprising because eukaryotic transcription factors are known to bind distal enhancers and, via multiprotein complexes, loop to the TSS to regulate pol II and gene transcription.^{15–17} Genome-wide de novo motif analyses were also performed in the sham/vehicle, isoproterenol, and TAC data sets, and the results are presented as sequence logos (Table IV in the Data Supplement).

Table 1. Motif Identification in the FoxO1 ChIP-Seq Data

	Motif	Best Guess	% Targets	% Background	P Value
Sham/Veh					
Promoter	ACTACAHTCCC	GFY	14.84	0.81	1.00E-130
	TTGTTTAC	FOXO3	10.87	1.97	1.00E-44
	HCAHTTCCGGYY	FLI1	35.06	17.64	1.00E-38
TSS	GGGADTTGTAGT	GFY	47.29	0.95	1e-658
	TTCCAGAAATGC	ZNF143	23.35	1.37	1.00E-205
	TGCCGGAA	ELK1	49	25.28	1.00E-57
In-gene	NBTGTTTACN	FOXO4	22.55	2.71	1.00E-129
	ACAGGAARYS	ERG	31.73	9.97	1.00E-77
	ACTACAATTCCC	GFY	3.98	0.32	1.00E-28
Intergenic	ACTACAATTCCC	GFY	19.98	0.83	1.00E-200
	HGTAAACA	FOXI1	14.13	1.47	1.00E-88
	SABTTCCGGY	FLI1	48.74	25.23	1.00E-56
Iso					
Promoter	ACTACAAYTCCC	GFY	16.6	0.8	1.00E-153
	GTAACAA	FOXO3	19.47	5.12	1.00E-55
	RRCCGGAAGT	ETV1	33.5	14.3	1.00E-50
TSS	GGGANNTGTAGT	GFY	53.96	1.14	1e-749
	TTCTGGGAAATG	STAT5A/B	23.67	1.36	1.00E-209
	GGCATTCTGG	ZNF143	41.83	10.02	1.00E-150
In-gene	DGTAAACA	FOXO4	34.33	6	1.00E-154
	ACTTCCTGY	ETS1	39.36	10.53	1.00E-121
	VBAACAATRG	SOX9	19.01	6.82	1.00E-35
Intergenic	ACTACAAYTCCC	GFY	21.36	0.74	1.00E-227
	TGTTTACD	FOXI1	22.48	3.31	1.00E-111
	CCGGAAGT	ETS	48.97	20.49	1.00E-86
TAC					
Promoter	ACTACAATTCCC	GFY	12.01	0.76	1.00E-98
	TGTAACARG	FOXO1	9.28	1.73	1.00E-37
	CTTCCGGT	ETS	48.44	30.95	1.00E-29
TSS	GGGANNTGTAGT	GFY	39.14	1.34	1e-446
	TTCCAGMATGC	ZNF143	15.82	0.98	1.00E-133
	TCSCGTAA	CEBPD	66.87	39.01	1.00E-70
In-gene	GTAACAACAVN	FOXO4	24.29	4.35	1.00E-103
	ACTTCCTG	ERG	44.59	20.32	1.00E-64
	AACAACAACA	FOXK1	16.33	7.45	1.00E-19
Intergenic	ACTACAATTCCC	GFY	16.38	0.83	1.00E-150
	GTAACAACVN	FOXO6	16.68	3.05	1.00E-68
	NACCGGAAGT	FLI1	41.35	17.69	1.00E-66

FoxO1 ChIP-Seq was performed as described in Figure 1. Sequences from the promoter, TSS, in-gene, and intergenic regions were used as input for identification of de novo motifs. The top 3 identified motifs are listed for each region for sham/vehicle, isoproterenol, or TAC. Also listed are the predicted binding proteins for each motif (Best Guess), the percentage of targets containing the listed motif (% Targets), the percentage of background sequences containing the listed motif (% Background), and the *P* value. ChIP-Seq indicates chromatin immunoprecipitation–deep sequencing; FoxO1, forkhead box protein; Iso, isoproterenol; TAC, transverse aortic constriction; TSS, transcription start site; and Veh, vehicle.

FoxO1 Aligns With pol II at the TSS of Genes

Because FoxO1 is detected primarily at the TSS of genes, we aimed to assess its role in the regulation of pol II

dynamics and gene expression. We therefore aligned our FoxO1 ChIP-Seq data with pol II ChIP-Seq data from murine hearts after sham operation or TAC for 7 days (Gene Expression Omnibus: GSE50637). The data demonstrate significant overlap between FoxO1 and pol II

binding at the TSS of genes after sham operation or TAC. Specifically, 97% and 75% of FoxO1-bound genes contain pol II in this region after sham and TAC, respectively (Figure 3A and 3B). In addition, pathway analyses of the overlapping genes show that those of the metabolic pathways were most represented (Tables V and VI in the Data Supplement). Overlap between FoxO1 and pol II bound to the TSS of genes was also observed at correlation coefficients for observed over expected values ($r=0.852$ and 0.824 in sham and TAC, respectively; Figure 3C and 3D). In contrast, promoter-distal and in-gene regions showed correlation coefficients for FoxO1 versus pol II that were relatively lower ($r=0.500$, 0.525 , 0.525 , and 0.554) for promoter sham, promoter TAC, in-gene sham, and in-gene TAC, respectively (Figure IXA through IXD in the Data Supplement). Notably, although there is an overall increase in FoxO1 binding at the TSS during TAC, there is an overall decrease in pol II binding in this region during hypertrophic growth (Figure 3E through 3H). Furthermore, these data demonstrate not only the overlap between FoxO1 and pol II at the TSS but also the extensiveness of FoxO1 binding. From Figure 3A and 3B, we calculate that 60.2% of cardiac-expressed genes contain FoxO1 at the TSS at baseline, a figure that increases to 91.3% after TAC. Thus, the data show that FoxO1 binding is widespread and aligns with pol II at the TSS of genes.

FoxO1 Binding Is Increased at the TSS in All Subsets of Genes Regulated by Pol II During Cardiac Hypertrophy

To continue investigating the role of TSS-bound FoxO1 in regulating pol II dynamics and gene expression, we examined FoxO1 binding in distinct subsets of genes regulated by pol II. Genes that are characterized by de novo pol II recruitment were defined as having an increase in pol II at the TSS and in-gene regions (>1) after TAC (Figure 4A and 4B). De novo pol II recruitment is associated with an upregulation of gene expression under these conditions.² Conversely, genes that are characterized by pol II loss have reduced pol II at the TSS and in-gene regions (<1) after TAC (Figure 4C and 4D). Pol II loss is associated with downregulation of gene expression under these conditions.² These 2 subsets of genes (upregulated and downregulated), however, represent only 5.94% and 2.22% of genes regulated during cardiac hypertrophic growth. The majority of genes (55.76%) are regulated by pol II pause-release, with another group (23.54%) being regulated by a combination of pol II de novo recruitment and pause-release (Table 2). Pol II pause-release genes are defined by reduced pol II at the TSS (<1) and unchanged or increased pol II at in-gene regions (≥ 1) after TAC (Figure 4E and 4F). Pol II pause-release is associated with incremental increases

in transcription and gene expression that match an increase in cardiomyocyte size.² Finally, the gene subset that is defined by pol II de novo recruitment and pause-release is characterized by an decrease in pol II at the TSS (<1) and an increase in pol II in the in-gene region (>1) after TAC (Figure 4G and 4H). This category is associated with an upregulation of gene expression under these conditions.² When we examined overall FoxO1 binding in each of these gene subsets, it was significantly increased (Figure 4A through 4H). However, a larger percentage of genes regulated by pol II pause-release or de novo recruitment plus pause-release contain FoxO1 (95.51% and 95.87%, respectively) versus de novo recruitment or pol II loss (79.28% and 71.89%, respectively; Table 2). It should also be noted that the majority of genes in any group have increased FoxO1 binding (78.23%, 69.48%, 93.55%, and 94.24% for pol II de novo recruitment, loss, pause-release, or de novo recruitment+pause-release, respectively) versus decreased binding (11.26%, 2.41%, 1.9%, and 1.55% for pol II de novo recruitment, loss, pause-release, or de novo recruitment+pause-release, respectively; Table 2). Overall, these data reveal that FoxO1 binding increases in all subsets of pol II-regulated genes during cardiac hypertrophy. This suggests that FoxO1 is not a defining factor for these gene categories but may play a role in the regulation of each subset.

FoxO1 Knockdown Prevents Hypertrophic Gene Expression and Cardiomyocyte Hypertrophy In Vitro

Next, we evaluated the role of FoxO1 in hypertrophic gene expression. We began by examining the groups of genes regulated by pol II de novo recruitment and pause-release because these represent the largest percentages of pol II-regulated genes during hypertrophy (Table 2). A representative gene regulated by both pol II de novo recruitment and pause-release, as defined above, is shown in Figure 5A. Catechol-O-methyltransferase domain containing 1 (*Comtd1*) is a putative catechol-O-methyltransferase that belongs to a family of enzymes that catalyze catecholamine degradation and are therefore critical in opposing catecholamine-induced stress.¹⁸ *Comtd1* has increased FoxO1 binding at the TSS, upstream, and in-gene regions after TAC (Figure 5A). We evaluated the expression of this gene in neonatal rat ventricular cardiomyocytes treated with endothelin-1 (Et-1) for 48 hours. Et-1 is a prototypical hypertrophic agonist previously implicated in pathological cardiac growth.¹⁹ As expected, we observed an increase (3.1-fold) in *Comtd1* mRNA levels with Et-1 treatment, which was prevented with pretreatment of cells with adenovirus expressing short hairpin (sh)RNA against FoxO1 (Figure 5B). Similarly, we examined the

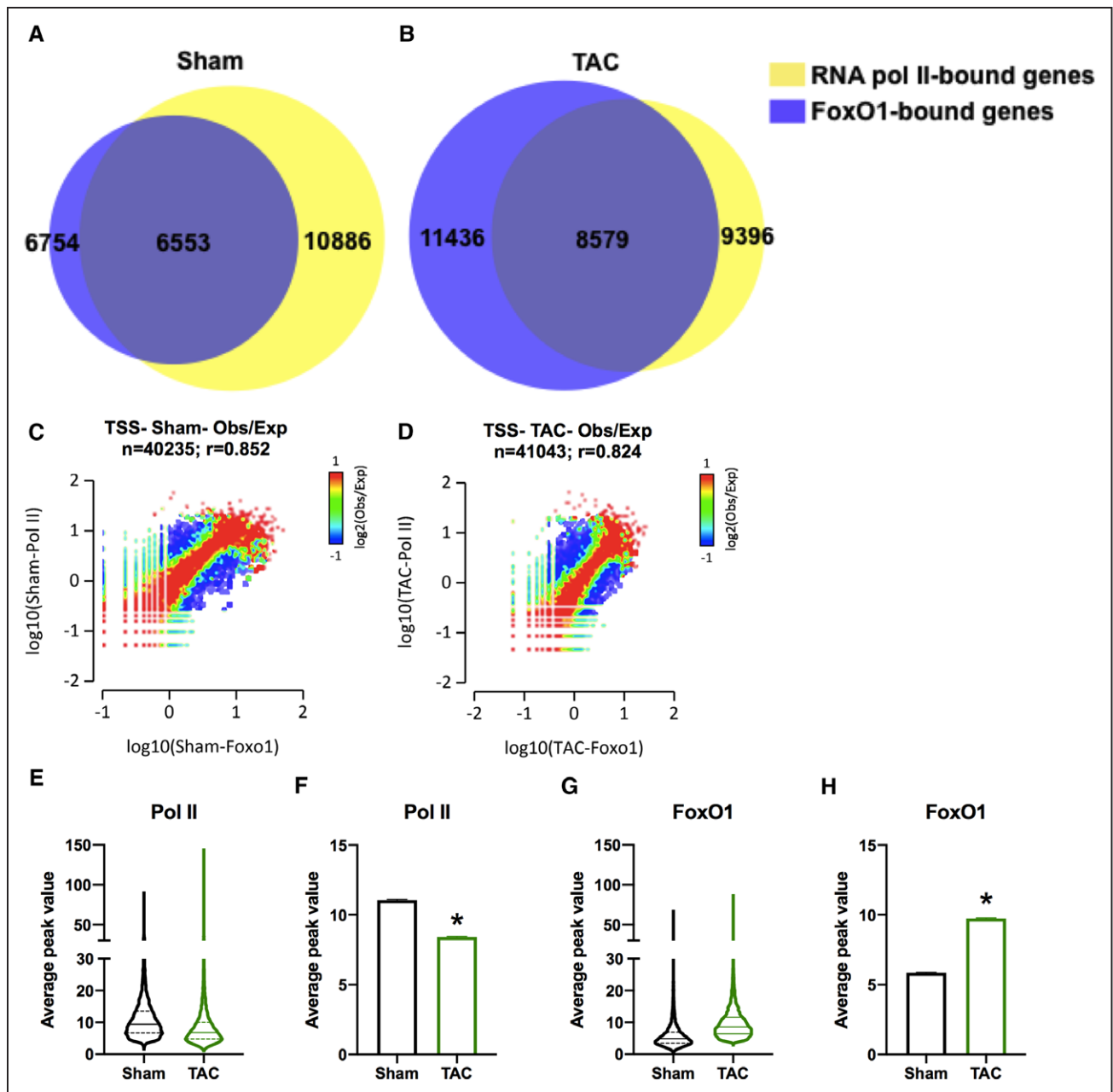


Figure 3. Forkhead box protein O1 (FoxO1) aligns with polymerase II (pol II) at the transcription start site (TSS).

FoxO1 and pol II chromatin immunoprecipitation followed by deep sequencing (ChIP-Seq) was performed in sham and transverse aortic constriction (TAC) hearts as described in Figure 1. **A** and **B**, Venn diagrams demonstrate the overlap between FoxO1-bound (blue) and pol II-bound (yellow) merged regions in sham (**A**) and TAC (**B**) hearts at the transcription start site (TSS). **C** and **D**, Two-dimensional histograms showing the distribution of fragments calculated from their overall frequencies in the ChIP-Seq of FoxO1 (x axis) vs Pol II (y axis) surrounding the TSS (–2000 to +2000 bp). The x and y axes were segmented into 75 bins, and the number of fragments within each bin was counted, color coded, and plotted. Bar to the **right** of the plot illustrates the relationship between count and coloring. Plots represent pseudo-colored 2D matrices showing observed/expected distribution, calculated from the overall frequencies of fragments on each of the axes. This plot shows the relation between FoxO1 and Pol II relative to what is expected if they occurred by chance. The pseudocolor corresponds to the observed-to-expected ratio (Obs/Exp), and the color intensity is proportional to the \log_{10} of the number of observed fragments within each bin. These plots suggest that there is a positive correlation between the binding of those 2 molecules, where red indicates that this occurs more frequently than expected by chance, as denoted by the correlation coefficient listed above the histogram. These figures were generated with EaSeq software. **E** through **H**, Average peak values for all merged regions of expressed genes (pol II sequencing tags >35 in sham or TAC at the TSS) containing FoxO1 (FoxO1 sequencing tags >35 in sham or TAC at the TSS) were plotted for pol II (**E**) or FoxO1 (**F**) at the TSS during sham or TAC. Data are presented as violin plots showing the median, quartiles, and distribution (**E** and **G**) or as bar graphs representing the mean (**F** and **H**). Error bars represent SEM. * $P<0.05$, TAC vs sham, t test.

expression of phosphoribosylformylglycinamide synthase (*Pfas*), a gene involved in de novo purine biosynthesis²⁰ and regulated by pol II pause-release, as defined above. *Pfas* also has increased FoxO1 binding at

the TSS, upstream, and in-gene regions after TAC (Figure 5C). As expected, there were no significant changes in *Pfas* mRNA levels with Et-1 treatment or FoxO1 shRNA expression (Figure 5D). Again, the reason is that

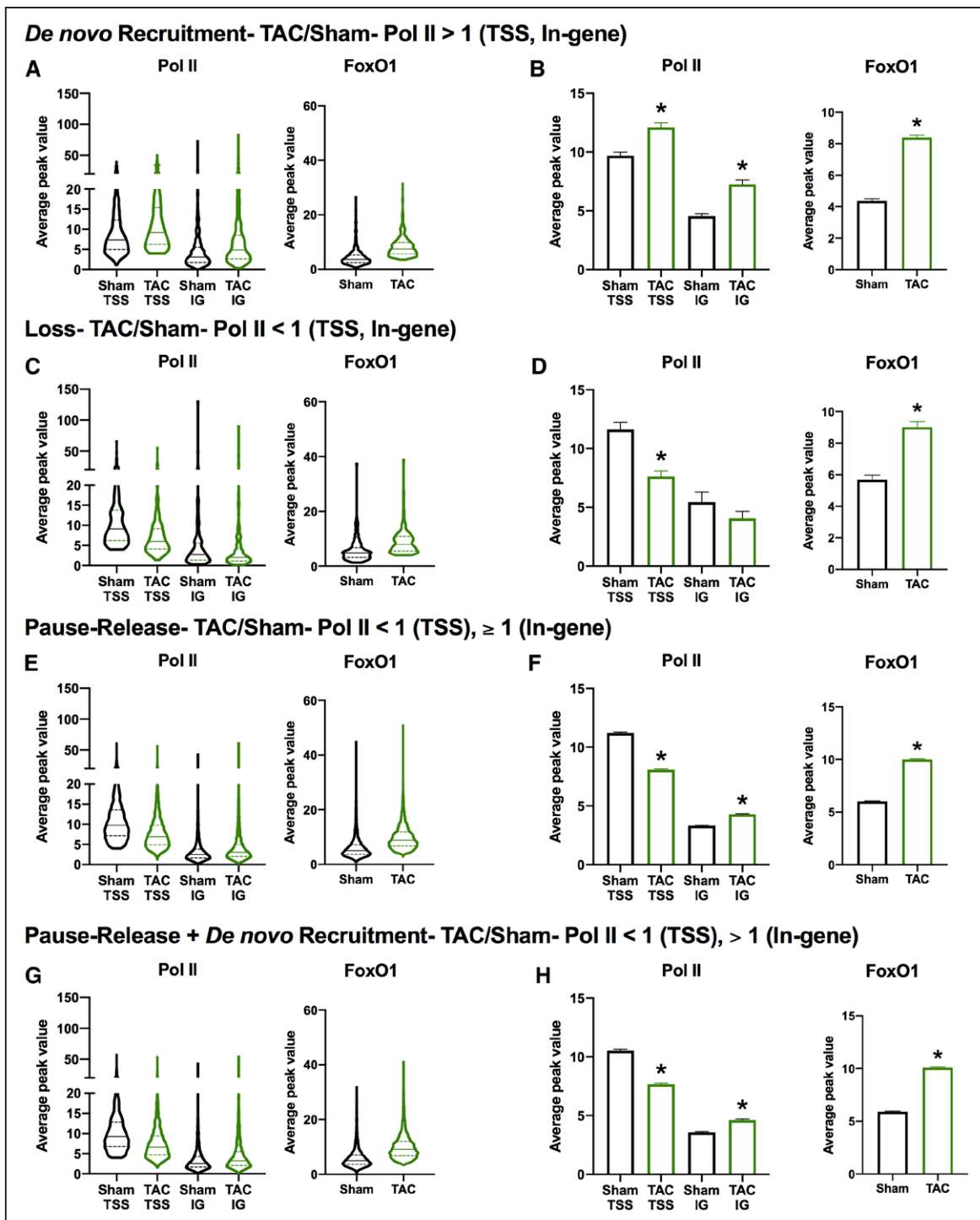


Figure 4. Forkhead box protein O1 (FoxO1) is increased at the transcription start site (TSS) in all subsets of genes regulated by polymerase II (pol II) during cardiac hypertrophy.

A through H, FoxO1 and RNA pol II chromatin immunoprecipitation followed by deep sequencing was performed in sham and transverse aortic constriction (TAC) hearts as described in Figure 1. Average peak values for all merged regions of expressed genes (pol II sequencing tags >35 in sham or TAC at the TSS) containing FoxO1 (FoxO1 sequencing tags >35 in sham or TAC at the TSS) were plotted for pol II (left) at the TSS or in-gene (IG) regions or FoxO1 (right) at the TSS during sham or TAC. Data are presented as violin plots showing the median, quartiles, and distribution (A, C, E, and G) or as bar graphs representing the mean (B, D, F, and H). Groups were defined as indicated. Error bars represent SEM. * $P < 0.05$, TAC vs sham, *t* test.

genes regulated by pol II pause-release have an increase in expression that matches an increase in cardiomyocyte size.² Thus, there are no apparent differences in expression via techniques that normalize to cellular size

such as quantitative polymerase chain reaction. Finally, we evaluated the role of FoxO1 in Et-1-induced hypertrophy in neonatal rat ventricular cardiomyocytes. As expected, Et-1 treatment for 24 hours increased

Table 2. Pol II–Regulated Gene Subsets During Cardiac Hypertrophy

	No. of Genes per Group	% of Total (11213 Genes)	No. of Genes per Group (FoxO1 Binding)	%	No. of Genes per Group (FoxO1 Increased)	%	No. of Genes per Group (FoxO1 decreased)	%
De novo recruitment	666	5.94	528	79.28	521	78.23	75	11.26
Loss	249	2.22	179	71.89	173	69.48	6	2.41
Pause-release	6252	55.76	5971	95.51	5849	93.55	119	1.90
Pause-release+de novo recruitment	2639	23.54	2530	95.87	2487	94.24	41	1.55

Gene subsets representing polymerase II (pol II) de novo recruitment (transverse aortic constriction [TAC]/sham-pol II >1 [transcription start site (TSS), in-gene]), loss (TAC/sham-pol II <1 [TSS, in-gene]), pause-release (TAC/sham-pol II <1 [TSS] and ≥1 [in-gene]), and pause-release+de novo recruitment (TAC/sham-pol II <1 [TSS] and >1 [in-gene]) are reported as numbers of genes per group of the overall expressed genes (pol II tags >35 at TSS in sham or TAC; 11 213 genes). The number of genes that bind FoxO1 (FoxO1 tags >35 at TSS in sham or TAC) for each group is also reported and displayed as percentages. Thirty-five was selected as a stringent cutoff because input DNA tags averaged 31 and 9 at the TSS in the pol II and FoxO1 chromatin immunoprecipitation–deep sequencing data sets, respectively. Of these FoxO1-bound genes, the number of genes per group with increased (TAC/sham-FoxO1>1) or decreased (TAC/sham-FoxO1<1) FoxO1 binding after TAC (number of genes per group [FoxO1 increased] or number of genes per group [FoxO1 decreased], respectively) was also reported and displayed with their respective percentages. FoxO1 indicates forkhead box protein.

cardiomyocyte size, an effect that is prevented with adenoviral expression of FoxO1 shRNA (Figure 5E and 5F). Together, these data suggest that FoxO1 may play a positive role in the regulation of pol II de novo recruitment and pause-release and therefore is critical in cardiomyocyte hypertrophic growth.

FoxO1 Knockdown Prevents Hypertrophic Gene Expression and Cardiomyocyte Hypertrophy In Vivo

Similar to what we observed in vitro, we show here that FoxO1 knockdown prevents pressure overload–mediated cardiac hypertrophic growth in vivo. Pretreatment of mice with adeno-associated virus (AAV) 9–expressing shRNA against FoxO1 (AAV.shFoxO1) normalized TAC-induced increases in cardiomyocyte cross-sectional area (Figure 6A and 6B) and partially prevented increases in HW/BW (Figure 6C) compared with scrambled control-expressing AAV9 (AAV.Scr). There are no significant changes in cardiac FoxO1 expression levels after TAC in AAV.Scr-treated control mice, and the extent of its knockdown is similar in AAV.shFoxO1–treated sham- or TAC-operated mice (29.8% and 33.3%, respectively; Figure 6D and 6E). Quantification of FoxO1 protein levels is normalized to cardiac α -actin, which does not bind appreciable amounts of FoxO1 (Figure 6F) and accordingly is not reduced with FoxO1 knockdown (Figure 6D). Similarly, α -actinin lacks detectable FoxO1 binding (Figure 6G) and is not altered with FoxO1 knockdown (Figure 6D). Conversely, *Gapdh*, which has considerable amounts of FoxO1 binding (Figure 6H), is decreased after FoxO1 knockdown (Figure 6D). Notably, after 2 (Figure XA and XB in the Data Supplement) or 9 (Figure XC and XD in the Data Supplement) days of AAV.Scr or AAV.shFoxO1 treatment, we do not observe any differences in cardiac function, as assessed by ejection fraction or fractional shortening. As shown,

we do not observe changes in cardiac function after 1 week of TAC versus sham-operated controls (Figures IA, IB, XC, and XD in the Data Supplement), and this is not altered with AAV.Scr or AAV.shFoxO1 treatment (Figure XC and XD in the Data Supplement). Moreover, aortic mean and peak pressure gradients were similar in sham-operated mice and equally increased after TAC between the AAV.Scr- (21.7-fold and 20.0-fold increased, respectively) and AAV.shFoxO1- (26.3-fold and 26.8-fold increased, respectively) treated groups (Figure XE and XF in the Data Supplement). A table with all major echocardiographic parameters, including heart rate, systolic and diastolic diameters, left ventricular (LV) mass, systolic and diastolic LV anterior wall thicknesses, and systolic and diastolic LV posterior wall thicknesses, is also included (Figure XG in the Data Supplement).

To examine the role of FoxO1 in the expression of pol II de novo recruitment- and pause-release–regulated genes in vivo, we measured their mRNA levels in murine hearts after TAC, with or without FoxO1 knockdown. FSTL1 (follistatin-related protein 1) is a cardiac-secreted glycoprotein that is increased in cardiomyocytes after TAC, where it prevents hypertrophic remodeling and subsequent failure.²¹ Uridine-cytidine kinase 2 is the enzyme that catalyzes the rate-limiting step of the pyrimidine-nucleotide biosynthetic salvage pathway.²² Both *Fstl1* and *Uck2* are regulated by pol II de novo recruitment after TAC, as observed by an increase in pol II binding, as described above (Figure 6I and 6J). These genes also have increased FoxO1 binding at their TSS and throughout their gene bodies (Figure 6I and 6J). As expected, this correlated with an increase in cardiac *Fstl1* and *Uck2* mRNA expression after TAC (3.1- and 2.0-fold, respectively) that was normalized with FoxO1 knockdown (Figure 6I and 6J). As negative controls, we measured the expression of genes that are regulated by pol II de novo recruitment during TAC but that do not bind considerable

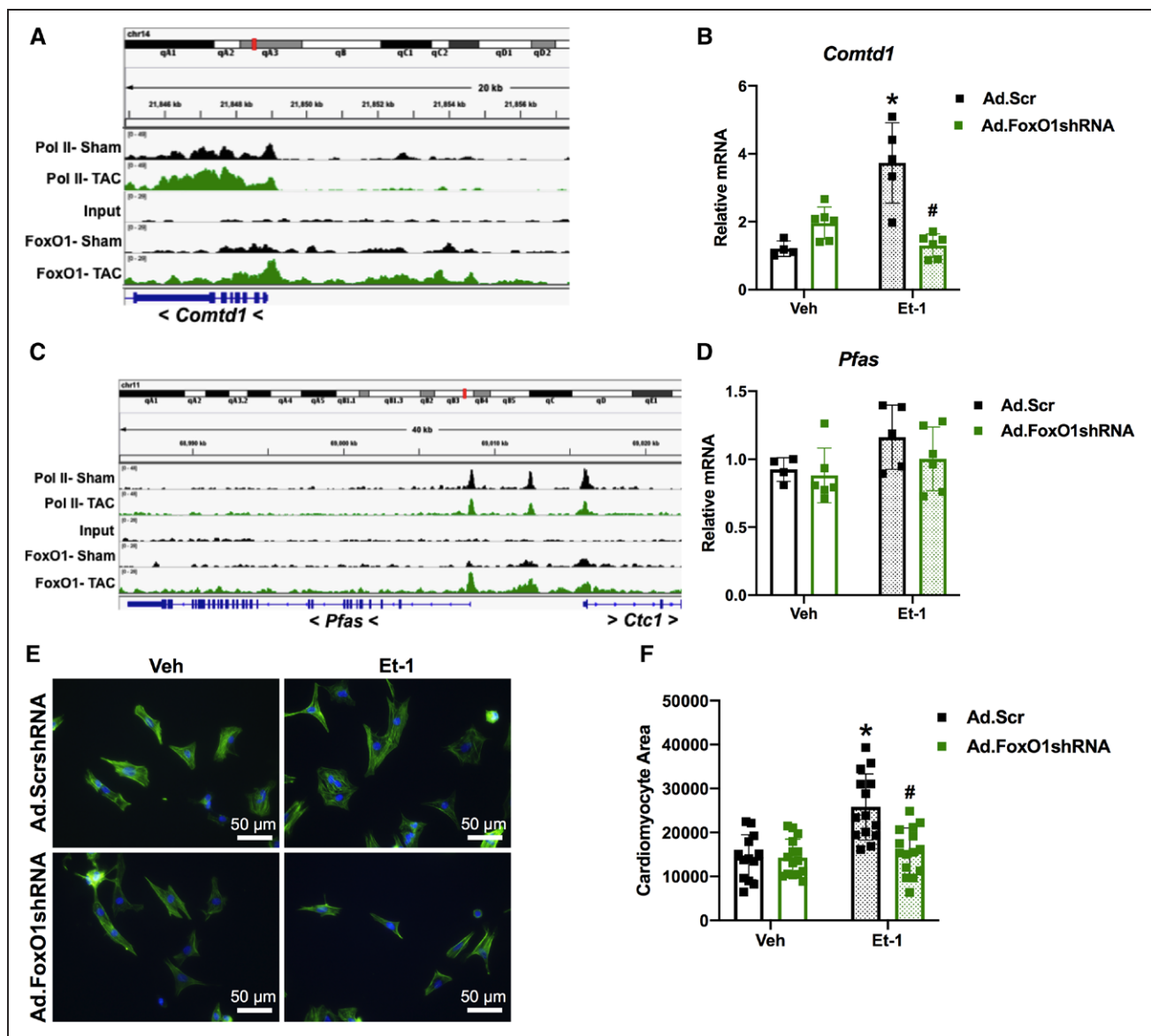


Figure 5. Forkhead box protein O1 (FoxO1) knockdown prevents hypertrophic gene expression and cardiomyocyte hypertrophy in vitro.

A through **D**, FoxO1 and RNA polymerase II (pol II) chromatin immunoprecipitation followed by deep sequencing was performed in sham and transverse aortic constriction (TAC) hearts as described in Figure 1. **A** and **C**, Integrated Genomics Viewer (IGV) software was used to view the fragment densities of pol II and FoxO1 (y axis) aligned along the gene coordinates (x axis). Shown are exemplary images for the indicated genes. **B** and **D** through **F**, Neonatal rat ventricular cardiomyocytes were treated with vehicle (Veh) or 100 nmol/L endothelin-1 (Et-1) and/or Ad.FoxO1shRNA or scrambled (Scr) control at a multiplicity of infection of 10 for 48 hours. **B** and **D**, Total RNA was extracted, and quantitative polymerase chain reaction was performed for the indicated genes. The results were plotted. $n=4, 5, 6$ (Veh, Et-1, Ad.FoxO1shRNA, Ad.FoxO1shRNA+Et-1). **E** and **F**, Cells were fixed and stained with 488 phalloidin (FITC) and DAPI. Representative images are shown in **E**. Cell area was quantified with ImageJ software and plotted (**F**). Cardiomyocytes imaged $n=13, 14, 15, 15$ (Veh/Ad.Scr, Veh/Ad.FoxO1shRNA, Et-1/Ad.Scr, Et-1/Ad.FoxO1shRNA). Error bars represent SEM. * $P<0.05$ vs Veh/Ad.Scr, # $P<0.05$ vs Et-1/Ad.Scr, 2-way ANOVA. Ad indicates adenovirus; and shRNA, short hairpin RNA.

amounts of FoxO1 such as natriuretic peptide A (*Nppa*) and actin- $\alpha 1$ (*Acta1*; (Figure XIA and XIB in the Data Supplement). As expected, there is an increase in the expression of these genes after TAC (7.1-fold and 7.9-fold, respectively), which is not normalized with FoxO1 knockdown. There is, however, a reduction in their expression, albeit nonsignificant, with FoxO1 knockdown, which is likely secondary to the partial rescue of cardiac hypertrophy (Figure XIA and XIB in the Data Supplement). Next, we examined genes that

are regulated by pol II pause-release after TAC such as *Psm5* and *Junb*. *Psm5* encodes a regulatory, non-ATPase subunit of the 26S proteasome,²³ whereas *Junb* is a transcription factor that has been shown to be upregulated 15 minutes after TAC but returns to baseline within 6 hours.²⁴ These genes also have increased FoxO1 binding at their TSS and throughout their gene bodies (Figure 6K and 6L). As expected, we did not see any changes in the expression of *Psm5* or *Junb* 7 days after TAC, nor did we detect any alterations with

FoxO1 knockdown (Figure 6K and 6L). Again, these data suggest that FoxO1 may positively regulate cardiac hypertrophic growth in vivo via positive regulation of pol II de novo recruitment and pause-release.

FoxO1 Deletion Prevents Cardiomyocyte Hypertrophy In Vivo

To corroborate our findings that AAV-mediated FoxO1 knockdown prevents pressure overload-induced cardiac hypertrophy, we measured cardiac hypertrophic growth in mice with cardiac-specific deletion of FoxO1 (FoxO1^{F/Fl,αMHC-Cre}). Mimicking our observations with AAV.shFoxO1 treatment, FoxO1 knockout prevented TAC-induced increases in cardiomyocyte cross-sectional area compared with controls (WT^{αMHC-Cre} or FoxO1^{F/Fl}; Figure 7A and 7B). Consistently, FoxO1 deletion prevented TAC-inducible increases in HW/BW versus controls (Figure 7C). Again, there were no significant changes in cardiac FoxO1 expression

levels after TAC compared with sham-operated controls, and the extent of FoxO1 knockout was similar in sham- and TAC-operated mice (40.8% and 43.7%, respectively) versus WT^{αMHC-Cre} controls (Figure 7D and 7E). Of note, we did not observe any differences in cardiac function, as assessed by ejection fraction and fractional shortening, at baseline (Figure XIA and XIIB in the Data Supplement) or 7 days after TAC (Figure XIIC and XIID in the Data Supplement). Moreover, aortic mean and peak pressure gradients were similar in sham-operated mice and equally increased after TAC (12.9-fold and 14.0-fold for WT^{αMHC-Cre}, 20.4-fold and 20.6-fold for FoxO1^{F/Fl}, and 16.3-fold and 16.9-fold for FoxO1^{F/Fl,αMHC-Cre}, respectively; Figure XIIE and XIIF in the Data Supplement). Tables with all major echocardiographic parameters, including heart rate, systolic and diastolic diameters, LV mass, systolic and diastolic LV anterior wall thicknesses, and systolic and diastolic LV posterior wall thicknesses, are also included (Figure XIIG in the Data Supplement).

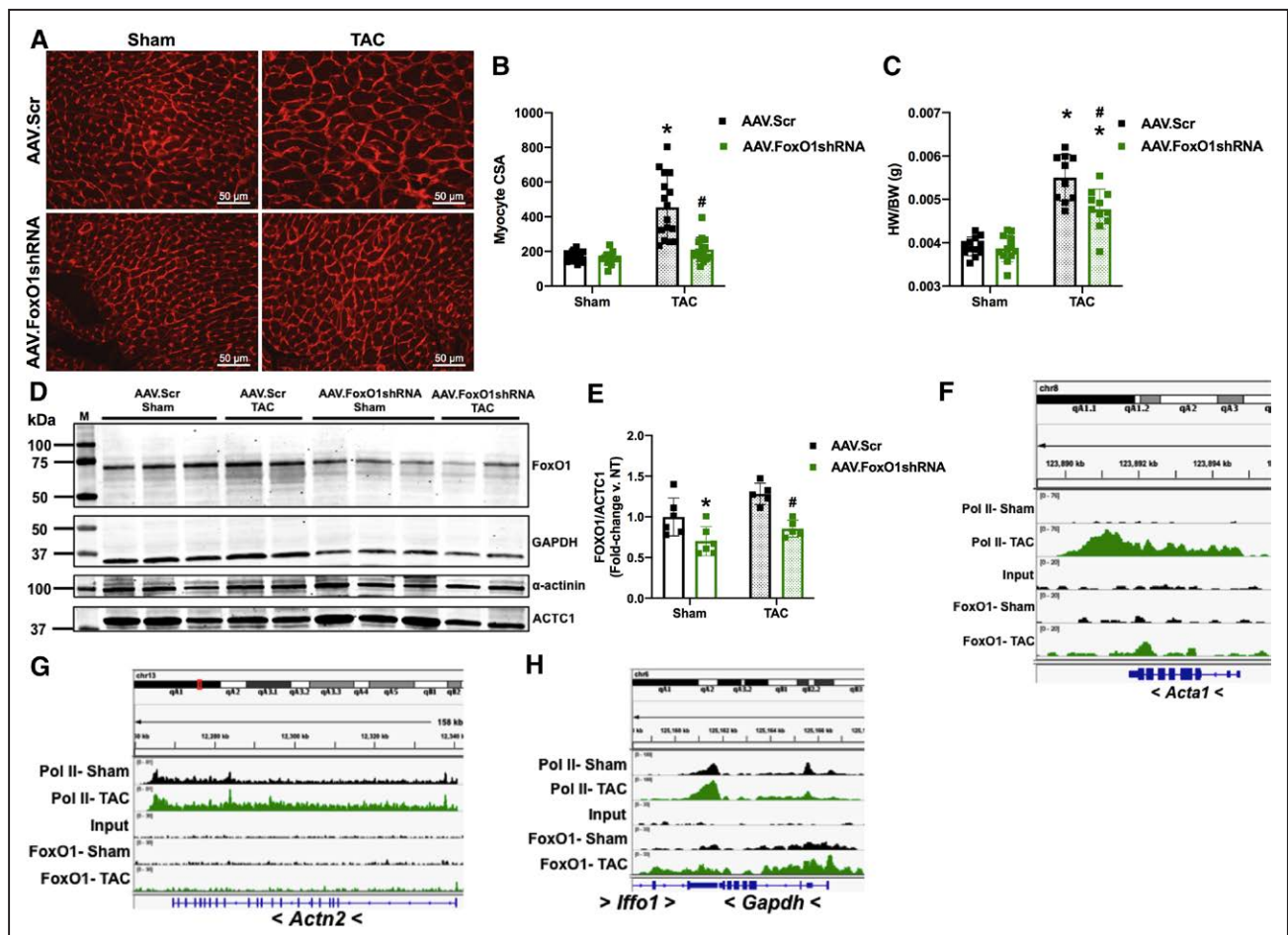


Figure 6. Forkhead box protein O1 (FoxO1) knockdown prevents hypertrophic gene expression and cardiomyocyte hypertrophy in vivo.

A through **E** and **I** through **L**, Adult (12-week-old) male mice were injected with adeno-associated virus (AAV).Scr or AAV.FoxO1shRNA (1×10^{12} GC/mL) for 2 days and then subjected to transverse aortic constriction (TAC) or sham surgery for 7 days. **A** and **B**, Hearts were harvested, fixed, and stained with 594 wheat germ agglutinin. Representative images are shown in **A**. Cell cross-sectional area (CSA) was quantified with ImageJ software and plotted (**B**). Cardiomyocytes imaged $n=16, 16, 16, 16$ (Sham/AAV.Scr, Sham/AAV.FoxO1shRNA, TAC/AAV.Scr, TAC/AAV.FoxO1shRNA). **C**, Hearts were harvested and weighed. Heart weights (HWs) were normalized to body weights (BW) and plotted as a ratio in grams. $n=12, 12, 10, 11$ (Sham/AAV.Scr, Sham/AAV.FoxO1shRNA, TAC/AAV.Scr, TAC/AAV.FoxO1shRNA). (Continued)

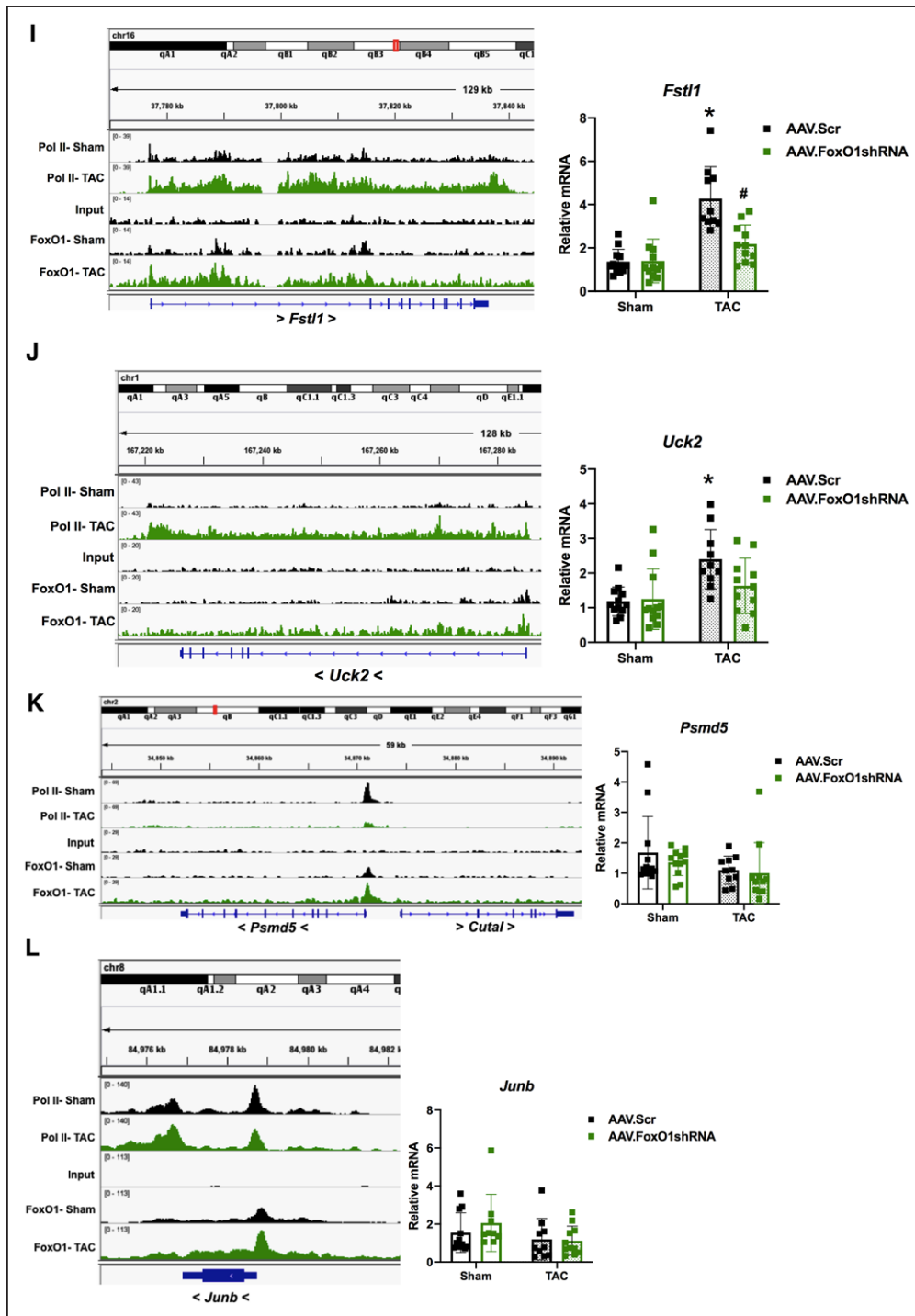


Figure 6 Continued. D and E, Hearts were harvested, lysed, and subjected to Western blotting with the indicated antibodies. Signals for FoxO1 were quantified with densitometry, normalized to the cardiac α -actin (ACTC1) loading control, and plotted. n=6, 6, 5 (Sham/AAV.Scr, Sham/AAV.FoxO1shRNA, TAC/AAV.Scr, TAC/AAV.FoxO1shRNA). F through L, FoxO1 and RNA polymerase II (pol II) chromatin immunoprecipitation followed by deep sequencing was performed in sham and TAC hearts as described in Figure 1. IGV software was used to view the fragment densities of pol II and FoxO1 (y axis) aligned along the gene coordinates (x axis). Shown are exemplary images for the indicated genes. I through L, Hearts were harvested; total RNA was extracted; and quantitative polymerase chain reaction was performed for the indicated genes. Results were plotted (right). n=12, 12, 10, 11 (*Fstl1*, *Uck2*, *Psm5*) and n=11, 9, 10, 11 (*Junb*; Sham/AAV.Scr, Sham/AAV.FoxO1shRNA, TAC/AAV.Scr, TAC/AAV.FoxO1shRNA). Error bars represent SEM. M indicates marker; Scr, Scrambled; and shRNA, short hairpin RNA. * $P < 0.05$ vs Sham/AAV.Scr, # $P < 0.05$ vs TAC/AAV.Scr, 2-way ANOVA.

DISCUSSION

FoxO1 was reported to be an atrophic transcription factor because it targets *Fbxo32*. Moreover, its

phosphorylation and nuclear export after adrenergic or angiotensin II receptor stimulation is prohypertrophic.^{8,13} On the other hand, our data uniquely show that in more long-term settings of hypertrophic stimulation

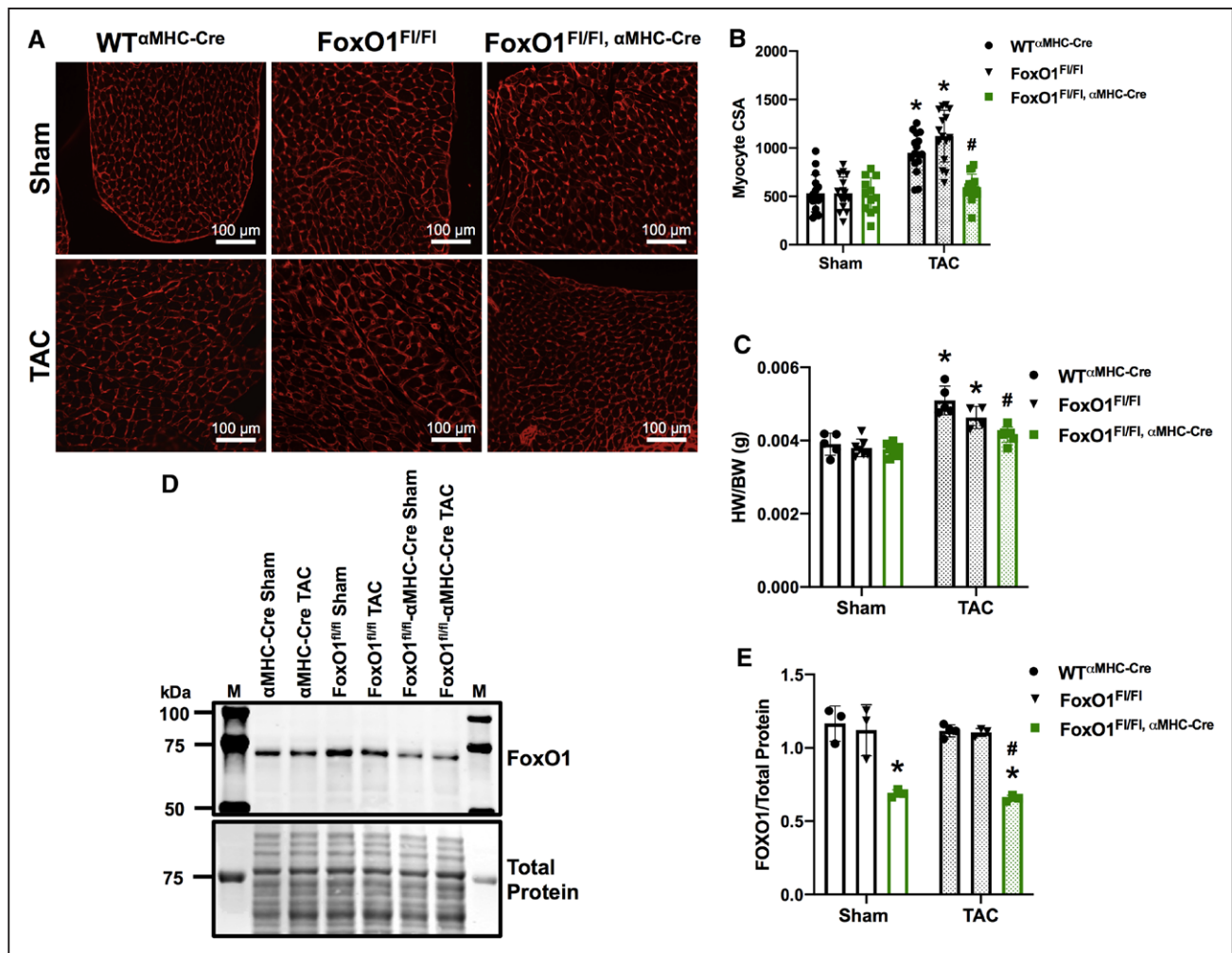


Figure 7. Forkhead box protein O1 (FoxO1) deletion prevents cardiomyocyte hypertrophy in vivo.

A through E. Adult (12-week-old) male WT α MHC-Cre, FoxO1^{FL/FL}, and FoxO1^{FL/FL} α MHC-Cre mice were subjected to transverse aortic constriction (TAC) or sham surgery for 7 days. **A and B.** Hearts were harvested, fixed, and stained with 594 wheat germ agglutinin. Representative images are shown in **A**. Cell cross-sectional area (CSA) was quantified with ImageJ software and plotted (**B**). Cardiomyocytes imaged $n=16, 16, 12, 16, 15, 16$ (WT α MHC-Cre-Sham, FoxO1^{FL/FL}-Sham, FoxO1^{FL/FL} α MHC-Cre-Sham, WT α MHC-Cre-TAC, FoxO1^{FL/FL}-TAC, and FoxO1^{FL/FL} α MHC-Cre-TAC). **C.** Hearts were harvested and weighed. Heart weights (HWs) were normalized to body weights (BW) and plotted as a ratio in grams. $n=5, 7, 9, 5, 4, 7$ (WT α MHC-Cre-Sham, FoxO1^{FL/FL}-Sham, FoxO1^{FL/FL} α MHC-Cre-Sham, WT α MHC-Cre-TAC, FoxO1^{FL/FL}-TAC, and FoxO1^{FL/FL} α MHC-Cre-TAC). **D and E.** Hearts were harvested, lysed, and subjected to Western blotting with the indicated antibody. Signals for FoxO1 were quantified with densitometry, normalized to total protein, and plotted. $n=3, 3, 3, 4, 3, 3$ (WT α MHC-Cre-Sham, FoxO1^{FL/FL}-Sham, FoxO1^{FL/FL} α MHC-Cre-Sham, WT α MHC-Cre-TAC, FoxO1^{FL/FL}-TAC, and FoxO1^{FL/FL} α MHC-Cre-TAC). Error bars represent SEM. α MHC indicates α -myosin heavy chain; M, marker; and WT, wild type. * $P<0.05$ vs WT α MHC-Cre-Sham, # $P<0.05$ vs WT α MHC-Cre-TAC, 2-way ANOVA.

such as 7 days of catecholaminergic- or pressure overload-induced stress, FoxO1 remains localized to the nucleus. One possibility is that FoxO1 nuclear export is uncoupled from upstream signaling, through G-protein coupled receptor kinase-dependent receptor desensitization.²⁵ Consistently, β -adrenergic receptor downregulation has been seen as early as 1 week after TAC.²⁶ Furthermore, FoxO1 phosphorylation and nuclear export are also observed after insulin receptor stimulation, a regulatory mechanism that is lost during conditions of insulin resistance or diabetes mellitus.²⁷

Although we did not find any significant alterations in cytosolic compared with nuclear localization of FoxO1 during cardiac hypertrophy, we did observe an overall increase in FoxO1 chromatin binding under these conditions. Consistently, we measured a

reduction in FoxO1 phosphorylation at serine 256, a site that, when phosphorylated, has been shown to reduce FoxO1-DNA binding affinity.¹⁴ Together, these data suggest that there is an unbound nuclear pool of FoxO1, which is not unprecedented for transcription factors and other transcriptional machinery. C-Fos, for example, is sequestered to the inner nuclear membrane during serum starvation via lamin A/C, which prevents its association with c-Jun and therefore the activity of this heterodimeric transcription factor, activating protein-1.²⁸ Another example is positive transcription elongation factor b (P-TEFb), which is composed of the cyclin-dependent kinase 9/cyclin T complex necessary for pol II phosphorylation and elongation.⁹ P-TEFb has been shown to bind hexamethylene bisacetamide-inducible proteins, which sequester it to small nuclear

RNA-protein complexes and inhibit its catalytic function.²⁹ Thus, it is possible that during cardiac hypertrophic stress, FoxO1 is released from nucleoplasmic or nuclear membranous pools to bind chromatin and regulate gene expression. It is also possible that ChIP-Seq is a more sensitive technique in detecting FoxO1 changes compared with tissue fractionation and Western blotting. However, we did confirm an increase in chromatin-bound FoxO1 in cardiomyocytes stimulated with isoproterenol for 48 hours via Western blotting, albeit with exogenous FoxO1 expression.

In addition to confirming an increase in FoxO1 chromatin binding in vitro, other steps were taken to ensure the high quality of our ChIP-Seq data. First, our ChIP was performed with a ChIP-Seq-validated antibody against FoxO1. The resultant data were then evaluated for the fraction of all reads that are present within peaks. Generally, the guidelines outlined by the ENCODE and modENCODE consortia specify that a fraction of reads in peaks >1% indicates reliable ChIP-Seq data.³⁰ The fractions of reads in peaks for our data were 5.3%, 2.3%, and 3.1% for sham/vehicle, isoproterenol, and TAC, respectively. The quality of the pol II ChIP-Seq antibody and data set was also confirmed.² In addition, our data were compared with FoxO1 ChIP-Seq performed in livers from WT and FoxO1 knockout mice.³¹ Notably, our peaks of FoxO1 enrichment overlapped with peaks found in genes that are also expressed in liver such as *Pdk4* (data not shown). These peaks were lost in the FoxO1 knockout mouse liver ChIP-Seq data.³¹ Finally, it should be noted that our data show increased FoxO1 binding in 2 independent models of cardiac hypertrophy, namely isoproterenol treatment and TAC, and that the extent of increase correlates well with extent of hypertrophy in these models. Thus, we are confident in the quality of our FoxO1 ChIP-Seq data and subsequent conclusions.

From these data, the majority of chromatin-bound FoxO1 was detected at the TSS of genes, where it aligns with pol II. Thus, we hypothesize its role in the regulation of pol II dynamics and gene expression. It is important to note that TSS-detected FoxO1 is likely caused by chromatin looping from promoter, in-gene, and intergenic genomic regions,^{15,17} as is supported by our motif analyses. This fact, however, does not affect our hypothesis about its function. Because FoxO1 binding is widespread and increases in genes regulated by pol II de novo recruitment, loss, and pause-release during hypertrophy, we speculated its role in the regulation of these subsets of genes. Not surprisingly, FoxO1 knockdown prevented the upregulation of *Comtd1*, *Fstl1*, and *Uck2*, which are genes that are regulated by pol II de novo recruitment and have increased FoxO1 binding during hypertrophy. Although FoxO1 also increases within genes regulated by pol II pause-release (ie, *Pfas*, *Psm5*, or *Junb*), the changes in their mRNAs are not

measurable because they increase incrementally in parallel with the increase in cellular size.² Their inhibition by FoxO1 knockdown or knockout, however, is reflected in the inhibition of Et-1- or TAC-induced increases in cardiomyocyte size in particular because these genes represent a relatively large fraction (55.8%) of the pol II-regulated genes after pressure overload compared with those regulated by de novo recruitment (5.9%; Table 2). It should be noted that *Comtd1*, *Fstl1*, and *Uck2* are exemplary genes regulated by pol II de novo recruitment and that *Pfas*, *Psm5*, and *Junb* are exemplary genes regulated by pol II pause-release. These are part of a much larger FoxO1-mediated gene program that represent hundreds and thousands of genes, respectively, of which the net effect of their transcriptional activation is prohypertrophic.

In terms of the mechanism, it is likely that FoxO1 indirectly regulates pol II and P-TEFb recruitment via intermediary molecules. Indirect recruitment may occur via molecules such as P300, FoxA1/2, or Brd4. P300 is a transcriptional coactivator with histone acetyltransferase activity, which has been shown to bind and acetylate FoxO1, with conflicting reports associating acetyl-FoxO1 with enhanced versus reduced transcriptional activity.^{32–34} P300 contains a bromodomain that recognizes acetylated lysine residues,³⁵ as well as directly binds pol II.³⁶ It is therefore possible that P300 mediates FoxO1-dependent recruitment of pol II during cardiac hypertrophy. The role of histone acetylation, via P300 or other histone acetyltransferases, and its interplay with FoxO1 and pol II recruitment have yet to be investigated and likely play a critical role. Notably, a recent set of studies demonstrate the requirement of FoxA1/2 binding to FoxO1 for chromatin relaxation and recruitment of pol II.^{37,38} Moreover, Brd4, another bromodomain-containing protein, has been shown to be required for FoxO1-mediated transcription in certain cancers.^{39,40} Thus, Brd4 may also play a role in FoxO1-dependent pol II recruitment during cardiac growth.

Although it is likely that FoxO1 indirectly regulates pol II or P-TEFb recruitment via molecules such as P300, FoxA1/2, or Brd4, its differential regulation of pol II de novo recruitment, loss, and pause-release is not understood. One possibility is that the protein complexes that contain FoxO1, pol II, and P-TEFb have varying compositions at differentially regulated loci. It is also possible that similar factors are involved but display temporal variation or differ in extent of binding. The elucidation of these crucial mechanistic details will allow us to specifically target cardiomyopathy genes compared with those that underlie adaptive growth.

Conclusions

Our study is the first to outline the full extent of transcriptional regulation by FoxO1 in the heart. We demonstrate

that through its regulation of a broad range of constitutively expressed genes, inhibition or loss of FoxO1 has the capacity to mitigate pressure overload–induced cardiac hypertrophic growth. We propose, however, that its utility as a therapeutic target for cardiac hypertrophy or failure requires further investigation because inhibiting the increase in cardiac mass would increase wall stress and thus would be counterproductive. In accordance, the genome-wide approach that we applied to this study underscores the necessity for comprehensively identifying the genomic bindings of transcriptional machinery and their rearrangements during disease, as well as the mechanisms by which they mediate their effects. This information will allow the design of more precise therapies to target transcription.

ARTICLE INFORMATION

Received February 24, 2020; accepted June 3, 2020.

The Data Supplement is available with this article at <https://www.ahajournals.org/doi/suppl/10.1161/circulationaha.120.046356>.

Correspondence

Jessica Pfleger, PhD, or Walter J. Koch, PhD, Center for Translational Medicine, Department of Pharmacology, Lewis Katz School of Medicine, Temple University, 3500 N Broad St, Philadelphia, PA 19140. Email jessica.pfleger@temple.edu or walter.koch@temple.edu

Affiliation

Center for Translational Medicine, Department of Pharmacology, Lewis Katz School of Medicine, Temple University, Philadelphia, PA.

Acknowledgments

The authors thank Dr Maha Abdellatif for kindly providing the adenoviruses.

Sources of Funding

This work was supported by the NIH (Grant Numbers: HL061690, HL075443, HL091799, and HL1346080 [to W.J.K.], HL139031 [to J.P.], and HL130218 and HL151924 [to K.D.]), the American Heart Association (Grant Number: 18MERIT33900036 [to W.J.K.]), and the American Heart Association and the Kahn Family Postdoctoral Fellowship in Cardiovascular Research (Grant Number: 18POST34060150 [to I.D.K.]). Dr Koch is the William Wikoff Smith Endowed Chair in Cardiovascular Medicine and a 2018 MERIT Awardee from the American Heart Association.

Disclosures

None.

Supplemental Materials

Expanded Methods
Data Supplement Figures I–XII
Data Supplement Tables I–VI
References 41–43

REFERENCES

- Taegtmeier H, Sen S, Vela D. Return to the fetal gene program: a suggested metabolic link to gene expression in the heart. *Ann NY Acad Sci*. 2010;1188:191–198. doi: 10.1111/j.1749-6632.2009.05100.x
- Sayed D, He M, Yang Z, Lin L, Abdellatif M. Transcriptional regulation patterns revealed by high resolution chromatin immunoprecipitation during cardiac hypertrophy. *J Biol Chem*. 2013;288:2546–2558. doi: 10.1074/jbc.M112.429449
- Sayed D, Yang Z, He M, Pfleger JM, Abdellatif M. Acute targeting of general transcription factor IIB restricts cardiac hypertrophy via selective inhibition of gene transcription. *Circ Heart Fail*. 2015;8:138–148. doi: 10.1161/CIRCHEARTFAILURE.114.001660
- Cao DJ, Wang ZV, Battiprolu PK, Jiang N, Morales CR, Kong Y, Rothermel BA, Gillette TG, Hill JA. Histone deacetylase (HDAC) inhibitors attenuate cardiac hypertrophy by suppressing autophagy. *Proc Natl Acad Sci USA*. 2011;108:4123–4128. doi: 10.1073/pnas.1015081108
- Ooi JY, Tuano NK, Rafehi H, Gao XM, Ziemann M, Du XJ, El-Osta A. HDAC inhibition attenuates cardiac hypertrophy by acetylation and deacetylation of target genes. *Epigenetics*. 2015;10:418–430. doi: 10.1080/15592294.2015.1024406
- Anand P, Brown JD, Lin CY, Qi J, Zhang R, Artero PC, Alaiti MA, Bullard J, Alazem K, Margulies KB, et al. BET bromodomains mediate transcriptional pause release in heart failure. *Cell*. 2013;154:569–582. doi: 10.1016/j.cell.2013.07.013
- Kim Y, Phan D, van Rooij E, Wang DZ, McAnally J, Qi X, Richardson JA, Hill JA, Bassel-Duby R, Olson EN. The MEF2D transcription factor mediates stress-dependent cardiac remodeling in mice. *J Clin Invest*. 2008;118:124–132. doi: 10.1172/JCI33255
- Ni YG, Berenji K, Wang N, Oh M, Sachan N, Dey A, Cheng J, Lu G, Morris DJ, Castrillon DH, et al. Foxo transcription factors blunt cardiac hypertrophy by inhibiting calcineurin signaling. *Circulation*. 2006;114:1159–1168. doi: 10.1161/CIRCULATIONAHA.106.637124
- Liu X, Kraus WL, Bai X. Ready, pause, go: regulation of RNA polymerase II pausing and release by cellular signaling pathways. *Trends Biochem Sci*. 2015;40:516–525. doi: 10.1016/j.tibs.2015.07.003
- Rasmussen EB, Lis JT. In vivo transcriptional pausing and cap formation on three Drosophila heat shock genes. *Proc Natl Acad Sci USA*. 1993;90:7923–7927. doi: 10.1073/pnas.90.17.7923
- Rougvie AE, Lis JT. The RNA polymerase II molecule at the 5' end of the uninduced hsp70 gene of *D. melanogaster* is transcriptionally engaged. *Cell*. 1988;54:795–804. doi: 10.1016/s0092-8674(88)91087-2
- Galbraith MD, Allen MA, Bensard CL, Wang X, Schwinn MK, Qin B, Long HW, Daniels DL, Hahn WC, Dowell RD, et al. HIF1A employs CDK8-mediator to stimulate RNAPII elongation in response to hypoxia. *Cell*. 2013;153:1327–1339. doi: 10.1016/j.cell.2013.04.048
- Zhang W, Yano N, Deng M, Mao Q, Shaw SK, Tseng YT. β -Adrenergic receptor-PI3K signaling crosstalk in mouse heart: elucidation of immediate downstream signaling cascades. *PLoS One*. 2011;6:e26581. doi: 10.1371/journal.pone.0026581
- Zhang X, Gan L, Pan H, Guo S, He X, Olson ST, Mesecar A, Adam S, Unterman TG. Phosphorylation of serine 256 suppresses transactivation by FKHR (FOXO1) by multiple mechanisms: direct and indirect effects on nuclear/cytoplasmic shuttling and DNA binding. *J Biol Chem*. 2002;277:45276–45284. doi: 10.1074/jbc.M208063200
- Meng H, Bartholomew B. Emerging roles of transcriptional enhancers in chromatin looping and promoter-proximal pausing of RNA polymerase II. *J Biol Chem*. 2018;293:13786–13794. doi: 10.1074/jbc.R117.813485
- Lambert SA, Jolma A, Campitelli LF, Das PK, Yin Y, Albu M, Chen X, Taipale J, Hughes TR, Weirauch MT. The human transcription factors. *Cell*. 2018;175:598–599. doi: 10.1016/j.cell.2018.09.045
- Kadauke S, Blobel GA. Chromatin loops in gene regulation. *Biochim Biophys Acta*. 2009;1789:17–25. doi: 10.1016/j.bbagr.2008.07.002
- Krakoff LR, Buccino RA, Spann JF Jr, De Champlain J. Cardiac catechol O-methyltransferase and monoamine oxidase activity in congestive heart failure. *Am J Physiol*. 1968;215:549–552. doi: 10.1152/ajplegacy.1968.215.3.549
- Suzuki T, Hoshi H, Mitsui Y. Endothelin stimulates hypertrophy and contractility of neonatal rat cardiac myocytes in a serum-free medium. *FEBS Lett*. 1990;268:149–151. doi: 10.1016/0014-5793(90)80995-u
- Mangold CA, Yao PJ, Du M, Freeman WM, Benkovic SJ, Szpara ML. Expression of the purine biosynthetic enzyme phosphoribosyl formylglycinamide synthase in neurons. *J Neurochem*. 2018;144:723–735. doi: 10.1111/jnc.14304
- Shimano M, Ouchi N, Nakamura K, van Wijk B, Ohashi K, Asaumi Y, Higuchi A, Pimentel DR, Sam F, Murohara T, et al. Cardiac myocyte follistatin-like 1 functions to attenuate hypertrophy following pressure overload. *Proc Natl Acad Sci USA*. 2011;108:E899–E906. doi: 10.1073/pnas.1108559108
- Suzuki NN, Koizumi K, Fukushima M, Matsuda A, Inagaki F. Crystallization and preliminary x-ray analysis of human uridine-cytidine kinase

2. *Acta Crystallogr D Biol Crystallogr*. 2003;59(Pt 8):1477–1478. doi: 10.1107/s0907444903011533
23. Shim SM, Lee WJ, Kim Y, Chang JW, Song S, Jung YK. Role of S5b/PSMD5 in proteasome inhibition caused by TNF- α /NF κ B in higher eukaryotes. *Cell Rep*. 2012;2:603–615. doi: 10.1016/j.celrep.2012.07.013
24. Rockman HA, Ross RS, Harris AN, Knowlton KU, Steinhelper ME, Field LJ, Ross J Jr, Chien KR. Segregation of atrial-specific and inducible expression of an atrial natriuretic factor transgene in an in vivo murine model of cardiac hypertrophy. *Proc Natl Acad Sci USA*. 1991;88:8277–8281. doi: 10.1073/pnas.88.18.8277
25. Choi DJ, Koch WJ, Hunter JJ, Rockman HA. Mechanism of beta-adrenergic receptor desensitization in cardiac hypertrophy is increased beta-adrenergic receptor kinase. *J Biol Chem*. 1997;272:17223–17229. doi: 10.1074/jbc.272.27.17223
26. Perrino C, Naga Prasad SV, Mao L, Noma T, Yan Z, Kim HS, Smithies O, Rockman HA. Intermittent pressure overload triggers hypertrophy-independent cardiac dysfunction and vascular rarefaction. *J Clin Invest*. 2006;116:1547–1560. doi: 10.1172/JCI25397
27. Aoyama H, Daitoku H, Fukamizu A. Nutrient control of phosphorylation and translocation of Foxo1 in C57BL/6 and db/db mice. *Int J Mol Med*. 2006;18:433–439.
28. Ivorra C, Kubicek M, González JM, Sanz-González SM, Alvarez-Barrientos A, O'Connor JE, Burke B, Andrés V. A mechanism of AP-1 suppression through interaction of c-Fos with lamin A/C. *Genes Dev*. 2006;20:307–320. doi: 10.1101/gad.349506
29. Kobbi L, Demey-Thomas E, Braye F, Proux F, Kolesnikova O, Vinh J, Poterszman A, Bensaude O. An evolutionary conserved Hexim1 peptide binds to the Cdk9 catalytic site to inhibit P-TEFb. *Proc Natl Acad Sci USA*. 2016;113:12721–12726. doi: 10.1073/pnas.1612331113
30. Landt SG, Marinov GK, Kundaje A, Kheradpour P, Pauli F, Batzoglou S, Bernstein BE, Bickel P, Brown JB, Cayting P, et al. CHIP-seq guidelines and practices of the ENCODE and modENCODE consortia. *Genome Res*. 2012;22:1813–1831. doi: 10.1101/gr.136184.111
31. Shin DJ, Joshi P, Hong SH, Mosure K, Shin DG, Osborne TF. Genome-wide analysis of FoxO1 binding in hepatic chromatin: potential involvement of FoxO1 in linking retinoid signaling to hepatic gluconeogenesis. *Nucleic Acids Res*. 2012;40:11499–11509. doi: 10.1093/nar/gks932
32. Perrot V, Rechler MM. The coactivator p300 directly acetylates the forkhead transcription factor Foxo1 and stimulates Foxo1-induced transcription. *Mol Endocrinol*. 2005;19:2283–2298. doi: 10.1210/me.2004-0292
33. Matsuzaki H, Daitoku H, Hatta M, Aoyama H, Yoshimochi K, Fukamizu A. Acetylation of Foxo1 alters its DNA-binding ability and sensitivity to phosphorylation. *Proc Natl Acad Sci USA*. 2005;102:11278–11283. doi: 10.1073/pnas.0502738102
34. Daitoku H, Sakamaki J, Fukamizu A. Regulation of FoxO transcription factors by acetylation and protein-protein interactions. *Biochim Biophys Acta*. 2011;1813:1954–1960. doi: 10.1016/j.bbamcr.2011.03.001
35. Mujtaba S, Zeng L, Zhou MM. Structure and acetyl-lysine recognition of the bromodomain. *Oncogene*. 2007;26:5521–5527. doi: 10.1038/sj.onc.1210618
36. Cho H, Orphanides G, Sun X, Yang XJ, Ogrzyko V, Lees E, Nakatani Y, Reinberg D. A human RNA polymerase II complex containing factors that modify chromatin structure. *Mol Cell Biol*. 1998;18:5355–5363. doi: 10.1128/mcb.18.9.5355
37. Schill D, Nord J, Cirillo LA. FoxO1 and FoxA1/2 form a complex on DNA and cooperate to open chromatin at insulin-regulated genes. *Biochem Cell Biol*. 2019;97:118–129. doi: 10.1139/bcb-2018-0104
38. Yalley A, Schill D, Hatta M, Johnson N, Cirillo LA. Loss of interdependent binding by the FoxO1 and FoxA1/A2 forkhead transcription factors culminates in perturbation of active chromatin marks and binding of transcriptional regulators at insulin-sensitive genes. *J Biol Chem*. 2016;291:8848–8861. doi: 10.1074/jbc.M115.677583
39. Gryder BE, Yohe ME, Chou HC, Zhang X, Marques J, Wachtel M, Schaefer B, Sen N, Song Y, Gualtieri A, et al. PAX3-FOXO1 establishes myogenic super enhancers and confers BET bromodomain vulnerability. *Cancer Discov*. 2017;7:884–899. doi: 10.1158/2159-8290.CD-16-1297
40. Nagarajan S, Bedi U, Budida A, Hamdan FH, Mishra VK, Najafova Z, Xie W, Alawi M, Indenbirken D, Knapp S, et al. BRD4 promotes p63 and GRHL3 expression downstream of FOXO in mammary epithelial cells. *Nucleic Acids Res*. 2017;45:3130–3145. doi: 10.1093/nar/gkw1276
41. Brinks H, Boucher M, Gao E, Chuprun JK, Pesant S, Raake PW, Huang ZM, Wang X, Qiu G, Gumpert A, et al. Level of G protein-coupled receptor kinase-2 determines myocardial ischemia/reperfusion injury via pro- and anti-apoptotic mechanisms. *Circ Res*. 2010;107:1140–1149. doi: 10.1161/CIRCRESAHA.110.221010
42. Martini JS, Raake P, Vinge LE, DeGeorge BR Jr, DeGeorge B Jr, Chuprun JK, Harris DM, Gao E, Eckhart AD, Pitcher JA, et al. Uncovering G protein-coupled receptor kinase-5 as a histone deacetylase kinase in the nucleus of cardiomyocytes. *Proc Natl Acad Sci USA*. 2008;105:12457–12462. doi: 10.1073/pnas.0803153105
43. Graham FL, Prevec L. Manipulation of adenovirus vectors. *Methods Mol Biol*. 1991;7:109–128. doi: 10.1385/0-89603-178-0:109